

MEDICAL IMAGING-A MATHEMATICAL APPROACH

Ms.Navneet Rana

PG Dept. of Mathematics,Guru Nanak College for Girls, Sri Muktsar Sahib (Punjab)

ABSTRACT

Mathematical models are used to interpret the measurement and a numerical algorithm to reconstruct an image. In modern medicine practice, there are various imaging techniques such as X-ray Computed Tomography (CT), Magnetic Resonance Imaging (MRI), Positron Emission Tomography (PET), Single Photon Emission Computed Tomography (SPECT) etc. These imaging techniques allow to create film images of objects and open the doors of non-invasive examination of interior condition of the human body.

This paper is an attempt to explain some mathematical methods beneficial in medical imaging (i.e. CT, MRI, PET). We will observe how human data from CT scan can be represented by Radon Transform. Unfiltered back projection is further a technique used to invert the Radon transform and explore the central slice theorem which connects the Radon and Fourier transforms. Unfiltered back projections for clarity and Filtered back projection method for inversion of Radon transform was used in reconstructing medical images. In MRI, Bloch phenomenological equation provide a model for the interaction between applied magnetic fields and the nuclear spins in the objects under consideration, partial Fourier reconstruction, parametric estimation are used. In case of PET, projection data kernel based image model is used and also maximum likelihood estimates is used for evaluating coefficients.

Key words: *Medical imaging, Radon transform, Fourier transform, Bloch equation.*

II. INTRODUCTION

Medical imaging is the technique and process of creating visual representations of the interior of a body for clinical analysis and medical intervention. Medical imaging seeks to reveal internal structures hidden by the skin and bones, as well as to diagnose and treat disease. Mathematical models are used to interpret the measurement and a numerical algorithm to reconstruct an image. In modern medicine practise, there are various imaging techniques such as X – ray Computed Tomography (CT), Magnetic Resonance Imaging (MRI), Positron Emission Tomography (PET), Single Photon Emission Computed Tomography (SPECT) etc. CT scans are very useful in diagnosis skeletal damage, cancer, tumour, vascular diseases and other abnormalities. . One can get more detailed information of human soft tissues with these techniques.

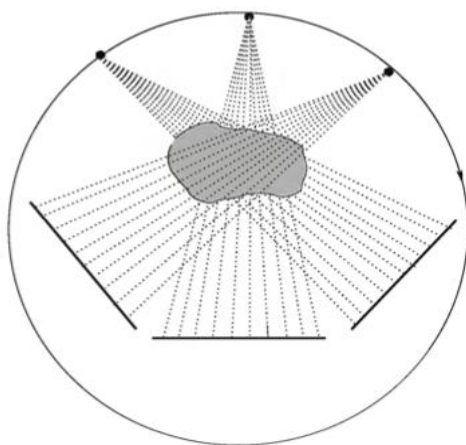
This paper is an attempt to explain some mathematical methods beneficial in Medical Imaging. CT is a diagnostic procedure that uses X –ray equipment by which the cross sectional image of the body is created. X-ray imaging is based on the absorption of X-rays that pass through the different parts of patient's body. X-ray transmission measurement are recorded on a computer memory device. The data is used to translate 2D external measurement into a reconstruction of 3D internal structure. This provides a numerical description of tissues

density or picture of a single thin slice through the body. Mathematical models and algorithms are developed for problems of image reconstruction.

A magnetic resonance imaging instrument (MRI scanner), or "nuclear magnetic resonance (NMR) imaging" scanner as it was originally known, uses powerful magnets to polarize and excite hydrogen nuclei (i.e. single protons) of water molecules in human tissue, producing a detectable signal which is spatially encoded, resulting in images of the body. The MRI machine emits a radio frequency (RF) pulse at the resonant frequency of the hydrogen atoms on water molecules. Radio frequency antennas ("RF coils") send the pulse to the area of the body to be examined. The RF pulse is absorbed by protons, causing their direction with respect to the primary magnetic field to change. When the RF pulse is turned off, the protons "relax" back to alignment with the primary magnet and emit radio-waves in the process. This radio-frequency emission from the hydrogen-atoms on water is what is detected and reconstructed into an image. The resonant frequency of a spinning magnetic dipole (of which protons are one example) is called the Larmor frequency and is determined by the strength of the main magnetic field and the chemical environment of the nuclei of interest. MRI uses three electromagnetic fields: a very strong (typically 1.5 to 3 Teslas) static magnetic field to polarize the hydrogen nuclei, called the primary field; gradient fields that can be modified to vary in space and time (on the order of 1 kHz) for spatial encoding, often simply called gradients; and a spatially homogeneous radio-frequency (RF) field for manipulation of the hydrogen nuclei to produce measurable signals, collected through an RF antenna.

Positron emission tomography (PET) is a nuclear medicine, functional imaging technique that produces a three-dimensional image of functional processes in the body. The system detects pairs of gamma rays emitted indirectly by a positron-emitting radionuclide (tracer), which is introduced into the body on a biologically active molecule. Three-dimensional images of tracer concentration within the body are then constructed by computer analysis. In modern PET-CT scanners, three dimensional imaging is often accomplished with the aid of a CT X-ray scan performed on the patient during the same session, in the same machine.

II. X-RAY IMAGING



- Figure 1.

A 2D diagram of a CT scanner. The CT scanner is made up of a point-source emitter and film that rotate around an object of interest, imaging the object in 2D slices and then compiling these slices into a 3D rendering of the object.

X-ray imaging relies on the principle that an object will absorb or scatter x-rays of a particular energy quantified by attenuation coefficient (μ). The intensity changes because of the attenuation coefficient of the object. This depends on the electron density of the substance.

Substances that are more dense and contain many electron have higher attenuation coefficient. As bones have a more attenuation coefficient than soft tissues and different soft tissues have different coefficient. Basic model for tomography is:

$dl / dx = - \mu (x) l$ where l is the intensity of x-ray beam and x is the arc length along the straight line trajectory of the x-ray beam.

Low energy (soft) x-rays are attenuated more efficiently than high energy (hard) x-rays. The distribution of energy is the output being skewed towards higher energies.

III.THE RADON TRANSFORM

J. Radon (1917), an Austrian mathematician introduced the theory of transform and integral operator. The Radon transform is widely applicable to Tomography. In CT one deals with the problem of finding a function $f(x)$ i.e. the tissue density at the internal point x . when $f(x)$ is found its density plot provides a picture (tomogram) with which doctor can look the internal structure of the patient. The approximation of the measurement of internal structure of an object is called 2-dimentional and Radon transform that takes the function on the plane and integrals it over all lines L is given by:

$$[f] \rightarrow Rf(L) = \int_L f(x,y)dl$$

one can determine line integral of the attenuation coefficient μ through the object by calculating from level of density. After taking these calculations for the full rotation it is possible to reconstruct the 2D slice of the object and compilation of multiple slices allows the 3D reconstruction of the object.

For work in the circular geometry of CT scans, it is suited to parameterize lines $ax+by=c$ in R^2 to a set of oriented lines with radical parameters $\ell_{t,\theta}$ in R^2 .

Let the vector $w = \langle \cos \theta, \sin \theta \rangle$ perpendicular to the line $ax+by=c$ and the vector $\hat{w} = \langle -\sin \theta, \cos \theta \rangle$ be parallel to this line. We get a vector equation in terms of t and θ for the line $\ell_{t,\theta} = tw + s\hat{w}$

$$= \langle t\cos \theta, t\sin \theta \rangle + s \langle -\sin \theta, \cos \theta \rangle$$

The line is same as $ax+by=c$ with the parameters t and θ as shown in the figure 2.

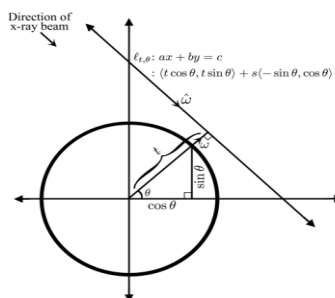


Figure 2

Definition: Let f be some function in \mathbb{R}^2 , parameterized over the lines $\ell_{t,\theta}$. The Radon transform $Rf(t,\theta)$ is defined as:

$$Rf(t,\theta) = \int_L f ds = \int_{-\infty}^{+\infty} f(t \cos \theta - s \sin \theta, t \sin \theta + s \cos \theta) ds$$

This definition describes the Radon transform for an angle θ . It accurately models the data acquired from taking cross-sectional scans of an object from a large set of angles, as in CT scanning, and its inverse can be used to reconstruct an object from CT data

Definition: Let f be some function in \mathbb{R}^2 , parameterized over the lines $\ell_{t,\theta}$. The unfiltered back-projection $B[f(t,\theta)]$ is defined as

$$B[f(t,\theta)] = \frac{1}{2\pi} \int_0^{2\pi} Rf(t,\theta) d\theta$$

Unfiltered back-projection is a simple and logical computation, but not a faithful representation of f . As unfiltered back-projection is not suitable for medical imaging applications because it portrays a blurry image. For inverting the Radon Transform, other method known as filtered back-projection is greatly applicable.

The Radon transform is closely related to the Fourier transform, a method whose inverse is well-described, by the Central Slice Theorem. In order to work in two-dimensional CT geometry, it is helpful to include an extension of the Fourier transform into two dimensions.

Definition: Let $f(x; y)$ be an absolutely integrable function. Then the two-dimensional Fourier transform is defined as:

$$\hat{f}(r,w) = \int_{-\infty}^{\infty} \int_{-\infty}^{\infty} f(x,y) e^{-iwr \cdot \langle x,y \rangle} dx dy$$

IV. THE CENTRAL SLICE THEOREM

connects both of the two transforms

Theorem: Let f be an absolutely integrable function in this domain. For any real number r and unit vector $w = (\cos \theta, \sin \theta)$

we have the identity

$$\hat{f}(r,w) = \int_{-\infty}^{\infty} Rf(t,\theta) e^{-itr} dt$$

From this theorem, we see that the 2-dimensional Fourier transform $\hat{f}(r,w)$ is equivalent to 1-dimensional Fourier transform of Radon transform $Rf(t,\theta)$. Filtered back-projection is a technique of inversion of Radon transform. This technique avoids the blurring artifact and lack of clarity in unfiltered back-projections. Mathematically, the method can be used to reduce the level of radiation exposure required to achieve the same level of diagnostic accuracy.

Several methods for inverting the Radon transform exist, some of which use Fourier transforms, the Central Slice Theorem, and functional analysis.

Definition: Given any integrable function F of t and θ , the transform R^* defines a function in x and y

$$R^*F(x,y) := \frac{1}{\pi} \int_0^\pi F(x \cos \theta + y \sin \theta, \theta) d\theta$$

The adjoint $R^*F(x, y)$ is equal to the average of $F(t, \theta)$ over the lines $\ell_{t,\theta}$ passing through the point (x,y) .

Proposition: A continuous function f equal to zero outside some disc and an integral function F of t and θ then

$$\langle Rf, F \rangle = \langle f, R^*F \rangle$$

Definition: The inverse Radon transform R^{-1} recover the function f from the Radon transform Rf of that function. This inversion is given by the formula:

$$f(x,y) = \lim_{z \rightarrow 0} \frac{1}{\pi} \int_0^\pi \int_{-\infty}^\infty Rf(t - x \cos \theta - y \sin \theta, \theta) \Gamma_z(t) dt d\theta \text{ where}$$

$$\Gamma_z(t) = \begin{cases} 1/\pi z^2 & \text{for } -z \leq t \leq z \\ 1/\pi z^2 (1 - 1/\sqrt{1 - z^2/t^2}) & \text{for } |t| > z \end{cases}$$

V. THE BLOCH EQUATION

The *Bloch phenomenological equation*, which provides a model for the interactions between applied magnetic fields and the nuclear spins in the objects under consideration. This is a macroscopic averaged model that describes the interaction of

aggregates of spins, called *isochromats*, with applied magnetic fields. Let $\mathbf{M}(t) = (M_x(t), M_y(t), M_z(t))$ be the nuclear magnetization. Then the Bloch equations read:

$$\begin{aligned} \frac{dM_x(t)}{dt} &= \gamma(\mathbf{M}(t) \times \mathbf{B}(t))_x - \frac{M_x(t)}{T_2} \\ \frac{dM_y(t)}{dt} &= \gamma(\mathbf{M}(t) \times \mathbf{B}(t))_y - \frac{M_y(t)}{T_2} \\ \frac{dM_z(t)}{dt} &= \gamma(\mathbf{M}(t) \times \mathbf{B}(t))_z - \frac{M_z(t) - M_0}{T_1} \end{aligned}$$

where γ is the gyromagnetic ratio and $\mathbf{B}(t) = (B_x(t), B_y(t), B_0 + \Delta B_z(t))$ is the magnetic field experienced by the nuclei. The z component of the magnetic field \mathbf{B} is sometimes composed of two terms:

- one, B_0 , is constant in time,
- the other one, $\Delta B_z(t)$, may be time dependent. It is present in magnetic resonance imaging and helps with the spatial decoding of the NMR signal.

$\mathbf{M}(t) \times \mathbf{B}(t)$ is the cross product of these two vectors. M_0 is the steady state nuclear magnetization (that is, for example, when $t \rightarrow \infty$); it is in the z direction.

In case of PET, projection data kernel based image model is used and also maximum likelihood estimates is used for evaluating coefficients.

VI. VARIOUS MEDICAL IMAGING TECHNIQUES

Like CT, MRI traditionally creates a two dimensional image of a thin "slice" of the body and is therefore considered a tomographic imaging technique. Modern MRI instruments are capable of producing images in the form of 3D blocks, which may be considered a generalization of the single-slice, tomographic, concept. Unlike CT, MRI does not involve the use of ionizing radiation and is therefore not associated with the same health hazards. For example, because MRI has only been in use since the early 1980s, there are no known long-term effects of exposure to strong static fields and therefore there is no limit to the number of scans to which an individual can be subjected, in contrast with X-ray and CT. However, there are well-identified health risks associated with tissue heating from exposure to the RF field and the presence of implanted devices in the body, such as pace makers. These risks are strictly controlled as part of the design of the instrument and the scanning protocols used.

With ordinary x-ray examinations, an image is made by passing x-rays through the patient's body. In contrast, nuclear medicine procedures use a radioactive material, called a radiopharmaceutical or radiotracer, which is injected into the bloodstream, swallowed or inhaled as a gas. This radioactive material accumulates in the organ or area of your body being examined, where it gives off a small amount of energy in the form of gamma rays. Special cameras detect this energy, and with the help of a computer, create pictures offering details on both the structure and function of organs and tissues in your body.

Because CT and MRI are sensitive to different tissue properties, the appearance of the images obtained with the two techniques differ markedly. In CT, X-rays must be blocked by some form of dense tissue to create an image, so the image quality when looking at soft tissues will be poor. In MRI, while any nucleus with a net nuclear spin can be used, the proton of the hydrogen atom remains the most widely used, especially in the clinical setting, because it is so ubiquitous and returns a large signal. This nucleus, present in water molecules, allows the excellent soft-tissue contrast achievable with MRI.

VII. CONCLUSION

The goal of this study is not to determine the overall best method but to present a study of some mathematical models and techniques used in medical imaging.

A few techniques used in medical imaging were studied and it was felt that from time to time new algorithms and new methods were developed and these improvements emerged the present form.

The original CT was developed for parallel geometry and then fan-beam geometries were used. Afterwards, the third generation scanners used cone beam and the current generation scanner are using spiral CT technology.

REFERENCES

1. Angenent, S., Pichon, E., & Tannenbaum, A. (2006). Mathematical methods in medical image processing. *Bulletin of the American Mathematical Society*, 43(3), 365-396.
2. Chan & Vese(2002). Active contour and segmentation models using geometric PDE's for Medical Imaging, *Geometric methods in biomedical image processing*, p-63-75.
3. Clack, R., & Defrise, M. (1994). Cone-beam reconstruction by the use of Radon transform intermediate functions. *JOSA A*, 11(2), 580-585.
4. Elbakri, I. A., & Fessler, J. A. (2002). Statistical image reconstruction for polyenergetic X-ray computed tomography. *IEEE Transactions on Medical Imaging*, 21(2), 89-99.
5. Epstein, Charles L. Introduction to the Mathematics of Medical Imaging. 2nd ed. Philadelphia, PA: Society for Industrial and Applied Mathematics, 2008. Print.
6. Jain, Anil K. (2013). Fundamentals of Digital Image Processing, PHI learning Pvt. Ltd, New Delhi
7. Freeman, T. G. (2010). The Mathematics of Medical Imaging. Springer Undergraduate Texts in Mathematics and Technology
8. Hiriyannaiah, H. P. (1997). X-ray computed tomography for medical imaging. *Signal Processing Magazine, IEEE*, 14(2), 42-59.
9. Katsevich, A. (2003). A general scheme for constructing inversion algorithms for cone beam CT. *International Journal of Mathematics and Mathematical Sciences*, 2003(21), 1305-1321.
10. Kuchment, P., & Lvin, S. (2013). Identities for $\sin x$ that Came from Medical Imaging. *The American Mathematical Monthly*, 120(7), 609-621.
11. Natterer, F. (1986). The Mathematics of computed Tomography. SIAM e-books.
12. Natterer, F. (1999). Numerical methods in tomography. *Acta Numerica*, 8, 107-141.
13. Natterer, F., & Ritman, E. L. (2002). Past and future directions in x-ray computed tomography (CT). *International Journal of Imaging Systems and Technology*, 12(4), 175-187.
14. Niervergelt, Yves. (1986). Elementary Inversion of Radon's Transform. *SIAM Review*, 28(1), 79-84.
15. Quinto, E. T. (2006). An introduction to X-ray tomography and Radon transforms. *In Proceedings of symposia in Applied Mathematics*, 63, 1.
16. Shepp, L. A., & Kruskal, J. B. (1978). Computerized tomography: the new medical X-ray technology. *American Mathematical Monthly*, 420-439.
17. Sidky, E. Y., Kraemer, D. N., Roth, E. G., Ullberg, C., Reiser, I. S., & Pan, X. (2014). Analysis of iterative region-of-interest image reconstruction for x-ray computed tomography. *Journal of Medical Imaging*, 1(3), 031007-031007.
18. Smith, K. T., & Keinert, F. (1985). Mathematical foundations of computed tomography. *Applied Optics*, 24(23), 3950-3957.
19. Tabbone, S., & Wendling, L. (2002). Technical symbols recognition using the two-dimensional radon transform. *In Proceedings 16th International Conference on Pattern Recognition*, IEEE, 3, 200-203.

20. Toft, P. A., & Sorensen, J. A. (1996). The Radon transform-theory and implementation (Doctoral dissertation, Technical University of Denmark, Center for Bachelor of Engineering Studies, Center for Information Technology and Electronics).of 3d whole-body pet/ct data using blurred Anatomical labels," phys med biol, vol. 47, pp. A. Abragam, Principles Of Nuclear Magnetism, Clarendon Press, Oxford,1983.
21. H. Barrett and K. J. Myers, foundations of image science, john wiley and sons, hoboken, 2004.
22. M. A. Bernstein, K. F. King, And X. J. Zhou, Handbook Of Mri Pulse Sequences, Elsevier Academic Press, London, 2004.
23. P. T. Callaghan, Principles Of Nuclear Magnetic Resonance Microscopy,Clarendon Press, Oxford, 1993.
24. P. T. Callaghan, 438 Nuclear Magnetic Resonance, Encyclopedia Of Mathematics And Physics, Elsevier, 2006.
25. C-N. Chen and D. I. Hoult, biomedical magnetic resonance technology,adam hilger, bristol, 1989.
26. A. Alessio, p. Kinahan, and t. Lewellen, "improved quantitation for pet/ct image reconstruction with system modeling and anatomical priors," spie med imaging, san Diego, 2005.
27. A. Alessio, p. Kinahan, and t. Lewellen, "modeling and incorporation of system response Functions in 3d whole body pet," submitted to ieee trans med imaging, 2005
28. H. H. Barrett, "objective assessment of image quality: effects of quantum noise and object Variability," j opt soc am a, vol. 7, pp. 1266-78, 1990.
29. C. Comtat, p. Kinahan, m. Defrise, c. Michel, and d. Townsend, "fast reconstruction of 3D PET data with accurate statistical modeling," ieee trans nuclear science, vol. 45, pp. 1083-1089, 1998.
30. C. Comtat, p. E. Kinahan, j. A. Fessler, t. Beyer, d. W. Townsend, m. Defrise, and c. Michel, "clinically feasible reconstruction 1-20, 2002